MODIS DATA STUDY
TEAM PRESENTATION

October 13, 1989

AGENDA

1. Status of the MODIS Data Study
2. Blackbody Radiances and the MODIS-N Thermal Bands
3. Chlorophyll Fluorescence Retrieval and Its Impact on Atmospheric Corrections
4. Some Issues Relating to Core MODIS Data Products, Algorithms, and Their Processing Scenario

MODIS DATA SYSTEM STUDY
APPROVAL
ACCOMP.

Summary of Deliverables

ORIG. APPVL. 06/24/88
LAST CHANGE 08/01/89
STATUS AS OF 10/01/89

	MILESTONES	89										90												91	
		M	A	M	J	J	A	S	O	N	D	J	F	M	A	M	J	J	A	S	O	N	D	J	F
01	Prel Data Requirements Doc																								
02	Non-Advocacy Review Materials																								
03	EosDIS/MIDACS I/F Comparison																								
04	Scenarios for Science Team																								
05	Prel TM Sci Prod Summary																								
06	Support MODIS Science Team Mtg																								
07	Input Data Attributes Report																								
08	MODIS Data Pkt Recommendation																								
09	Prel Core Prod Algorithm Rep																								
10	Prel TM Core Prod Analysis Rep																								
11	Core Data Proc Scenario Doc																								
12	Support MODIS Science Team Mtg																								
13	Prel MODIS Proc/Stor Req't Doc																								
14	Utility/Sup't Algo Req'ts Doc																								
15	MODIS SDST/ICT Requirem'ts Doc																								
16	Core Product Requirements Doc																								
17																									
18																									
19																									
20																									

Note: 1 - Draft Delivered

BLACKBODY RADIANCES AND THE MODIS-N THERMAL BANDS

Figure 1 illustrates the Planck blackbody irradiances for a moderate range of surface temperatures. In obtaining these irradiances, the Planck function (Equation 1) was evaluated at the center of each band.

$$(1) \quad L(\lambda,T) = \pi \, \epsilon(\lambda) \, 2hc^2 \, / \, [\lambda^5 \, (e^{hc \, / \, k\lambda T)} - 1)]$$

The temperatures correspond to a -13°C snow covered surface through a 37°C land surface at noon. The shortwave cutoff is present at around 3λm, as is the peak emission at 10μm. The characteristic behavior of the spectral irradiance distribution with increasing temperature is evident. Figure 2 presents the blackbody emission curves for elevated temperatures characteristic of forest fires/biomass burning and volcanic activity. The peak emission has increased by a factor of 100 and decreased in wavelength to 4 or 5 μm.

Table 1 presents the spectral radiances for each of the 16 MODIS-N thermal bands (in units of $Wm^{-2}\mu m^{-1}steradian^{-1}$) as a function of temperature. The radiances are computed for a range of temperatures and implicitely assume a blackbody surface and an optically inactive atmosphere. For most channels, a realistic temperature range is 220 to 330K. However, four of the MODIS thermal bands will be equipped with bilinear gains to permit the observation of surface fires and volcanic activity without seriously degrading other temperature measurements. For these channels, radiances for a range from 300K to 700K are presented.

Figure 3 graphically depicts the MODIS spectral radiance measurements for three surface temperatures. The abscissa is the specral band number, while the central wavelength (to 0.01μm) is presented above each radiance. As stated earlier, these estimates are valid at the band center and should be interpreted as effective blackbody emissions. For an atmospheric window region, e.g. at 4 or 12 μm, the effective temperatures will correspond closely to the product of the surface temperature and emissivity. Figures 4 and 5 are similar depictions for the four high-range bands (for linear and logarithmic ordinates.

Of course, a number of constituents in the atmosphere are optically active in many of the MODIS-N thermal bands. This effect is illustrated in Figure 6 for a 288K surface temperature (global mean) and for the standard atmosphere. LOWTRAN6 was used for the computation of the atmospheric absorption. The computation was performed for every 10 wavenumbers, which corresponds to about 0.6 μm near 25 μm and 0.04 μm near 2.0 μm. The radiative transfer package averages over 20 wavenumbers, which eliminate much of the fine spectral structure of the atmospheric absorption. Absorption features are clearly evident, including the 4.2 to 4.4 μm CO_2 band, the 5.5 to 7.3 μm H_2O band, the 9.5 to 10 μm O_3 band, the 13 to 16 μm CO_2 band, and the H_2O absorption for wavelengths greater than 16μm. Only at the 4 and 12 μm windows does the atmospheric transmissivity approach 100% and do the top of the atmosphere and bottom of the atmosphere curves agree.

Figure 7 overlays the 288K/standard atmosphere radiances (normalized to unity) on top of the band passes for the 16 thermal channels. The band passes are modelled as Gaussian curves (Equation 2) with 100% responses at the band centers (λo) and 50% responses at the band edges (full-width half maximum, or $\Delta\lambda$), as shown in Figure 8.

$$(2) \quad R(\lambda,T) = a\ e^{-b(\lambda-\lambda o)^2}$$

where $a = 1$

and $b = -4\ \ln(0.5)/(\Delta\lambda)^2$

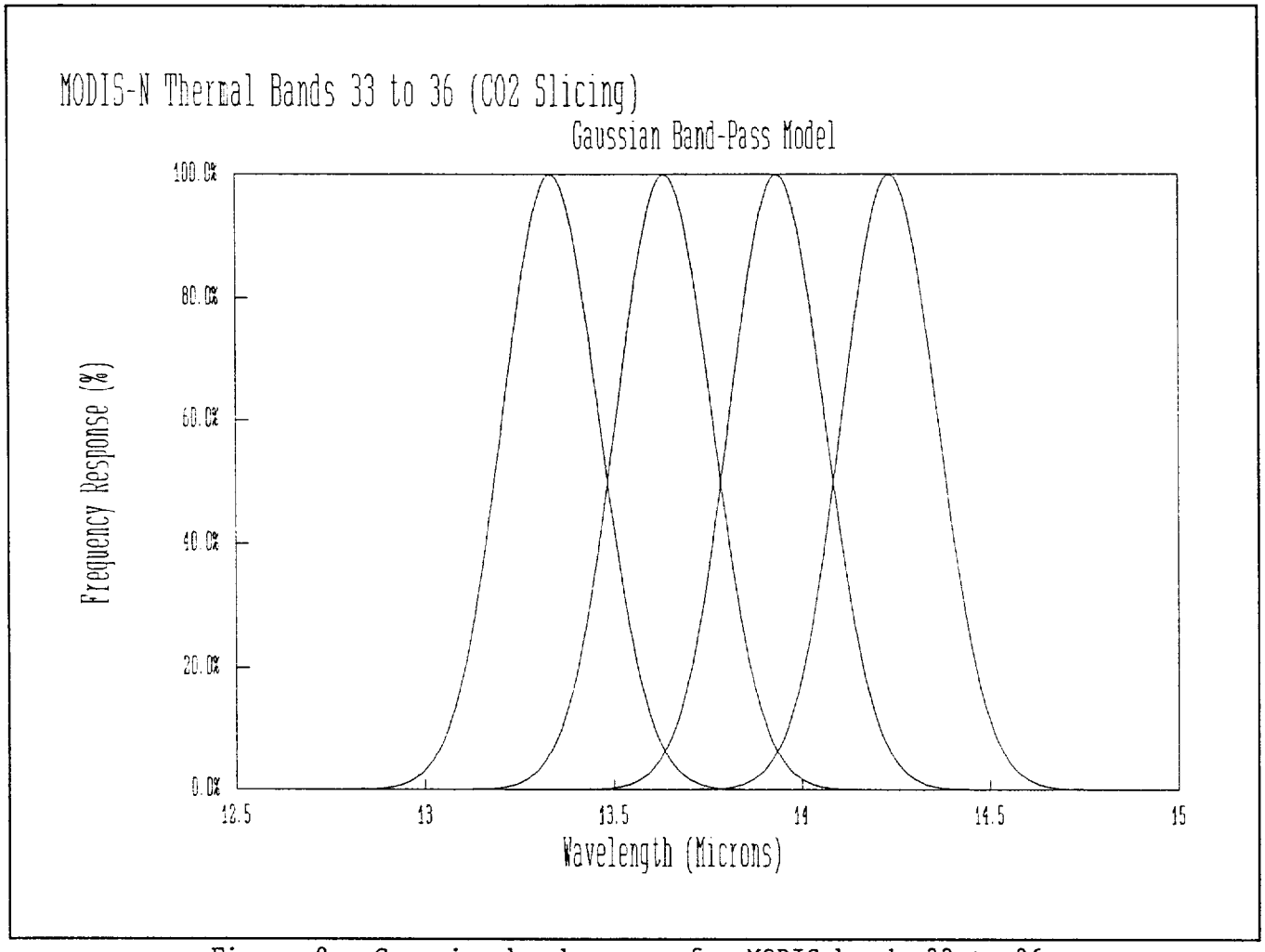

Figure 8. Gaussian band passes for MODIS bands 33 to 36.

The primary purpose of each band is presented in Table 2, and can generally be deduced from the absorption features illustrated in Figure 7.

MODIS Spectral Radiances (W/m^2/micron/steradian)

Channel	Center	Width	220	230	240	250	260	270	280	290	300	310	320	330
21	3.750	0.18	0.00	0.01	0.02	0.03	0.06	0.11	0.18	0.29	0.45	0.68	1.00	1.43
22	3.959	0.05	0.01	0.02	0.03	0.06	0.10	0.17	0.28	0.44	0.67	0.99	1.43	2.02
23	4.050	0.05	0.01	0.02	0.04	0.07	0.13	0.21	0.34	0.52	0.79	1.15	1.65	2.31
24	4.465	0.05	0.03	0.06	0.10	0.17	0.28	0.44	0.67	1.00	1.45	2.05	2.84	3.85
25	4.515	0.05	0.03	0.06	0.11	0.18	0.30	0.48	0.72	1.07	1.55	2.18	3.00	4.06
26	4.565	0.05	0.04	0.07	0.12	0.20	0.33	0.51	0.78	1.14	1.64	2.31	3.17	4.27
27	6.715	0.36	0.51	0.78	1.16	1.65	2.30	3.12	4.14	5.39	6.90	8.69	10.78	13.21
28	7.325	0.30	0.75	1.10	1.58	2.19	2.96	3.91	5.07	6.46	8.10	10.00	12.19	14.68
29	8.550	0.30	1.24	1.73	2.35	3.11	4.03	5.12	6.40	7.87	9.55	11.44	13.56	15.90
30	9.730	0.30	1.65	2.20	2.88	3.69	4.63	5.71	6.95	8.33	9.88	11.58	13.44	15.46
31	11.030	0.50	1.94	2.51	3.18	3.95	4.83	5.82	6.91	8.12	9.43	10.85	12.38	14.01
32	12.020	0.50	2.06	2.61	3.24	3.95	4.75	5.64	6.60	7.65	8.78	9.99	11.27	12.62
33	13.335	0.30	2.09	2.59	3.15	3.77	4.45	5.19	5.99	6.84	7.74	8.70	9.70	10.74
34	13.635	0.30	2.09	2.57	3.11	3.71	4.37	5.07	5.83	6.64	7.50	8.40	9.34	10.33
35	13.935	0.30	2.08	2.55	3.07	3.65	4.27	4.95	5.67	6.44	7.26	8.11	9.00	9.92
36	14.235	0.30	2.06	2.52	3.02	3.57	4.18	4.82	5.51	6.24	7.01	7.82	8.66	9.53

Channel	Center	Width	300	400	500	600	700
21-High	3.750	0.18	0.45	10.96	74.66	268.26	668.81
29-High	8.550	0.30	9.55	38.81	90.03	157.77	235.52
31-High	11.030	0.50	9.43	27.97	53.70	82.96	113.17
32-High	12.020	0.50	8.78	23.81	43.32	64.56	85.85

[Computed at center of band]

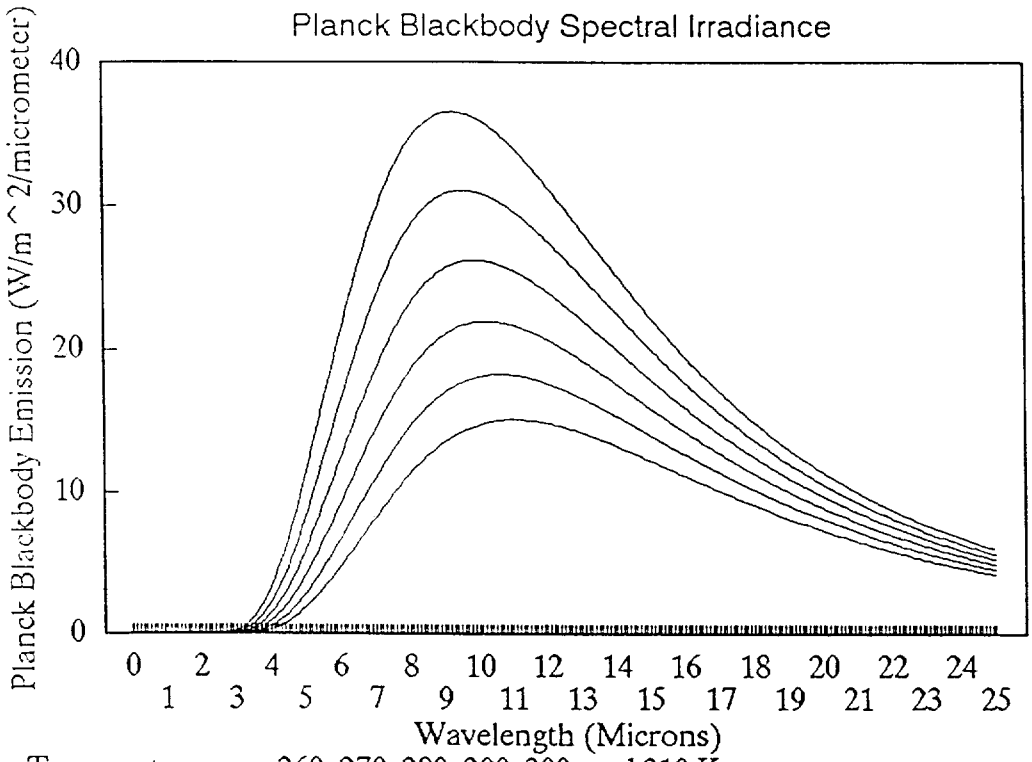

Temperatures are 260, 270, 280, 290, 300, and 310 K

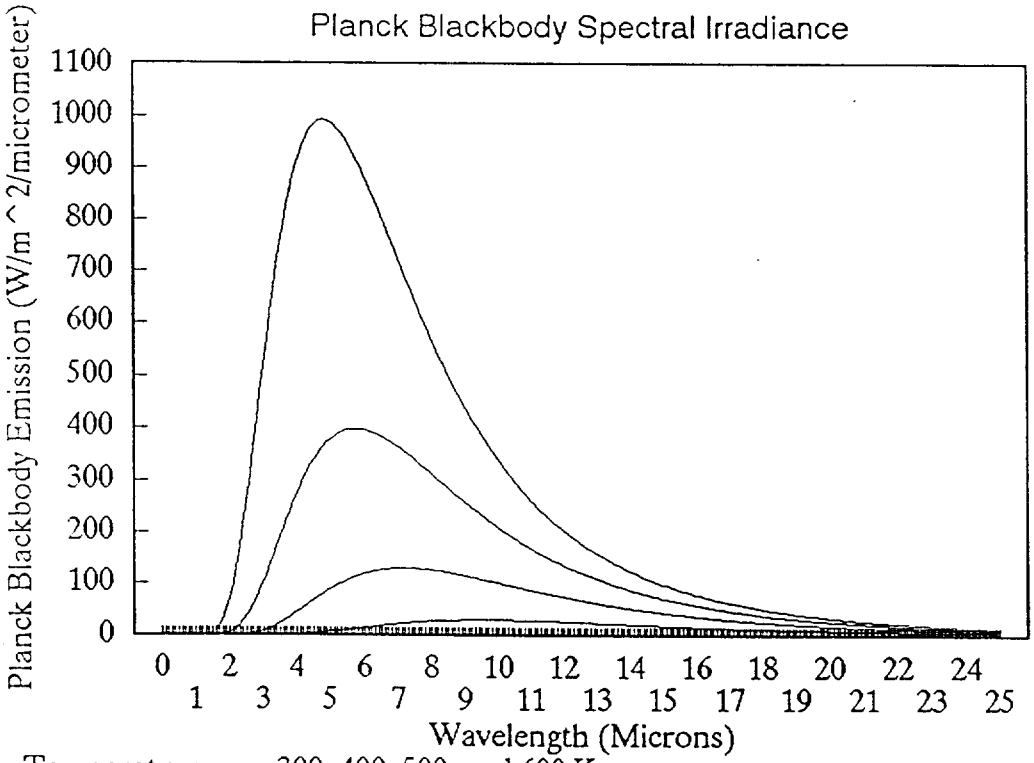

Temperatures are 300, 400, 500, and 600 K

MODIS Spectral Radiance Measurements

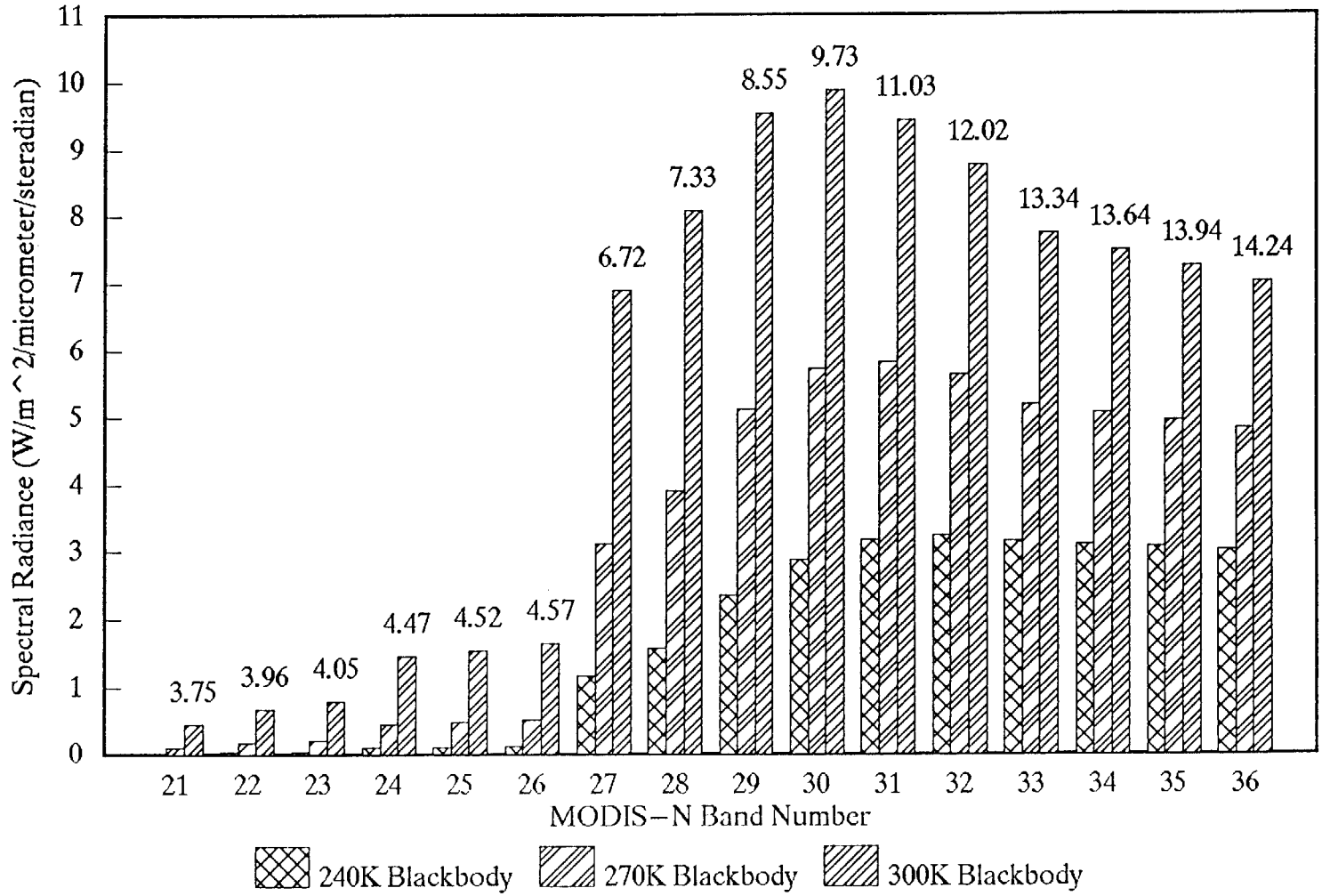

Temperatures are 240, 270, and 300K.

[Computed at center of band]

MODIS Spectral Radiance Measurements

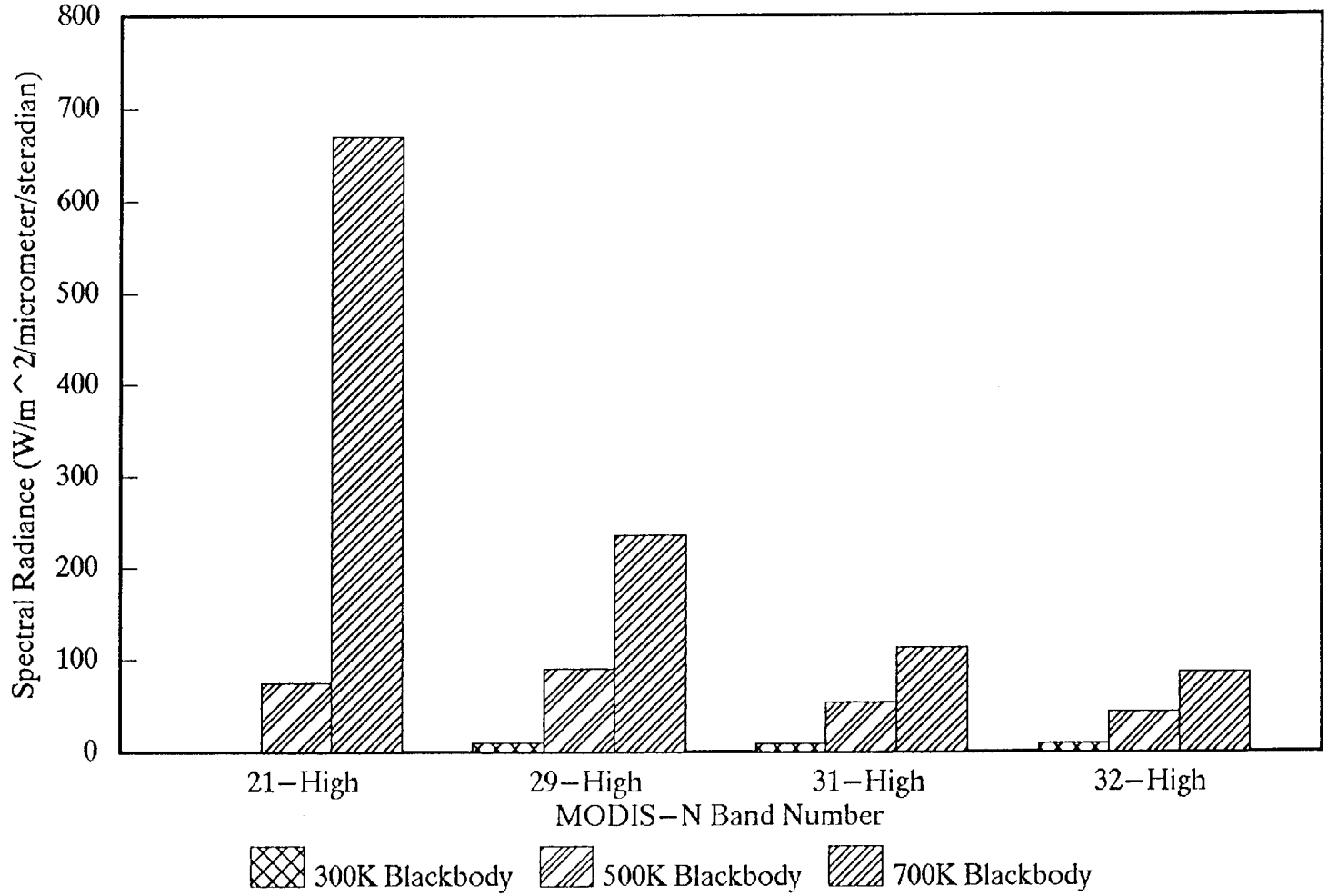

Temperatures are 300, 500, and 700K.

[Computed at center of band]

MODIS Spectral Radiance Measurements

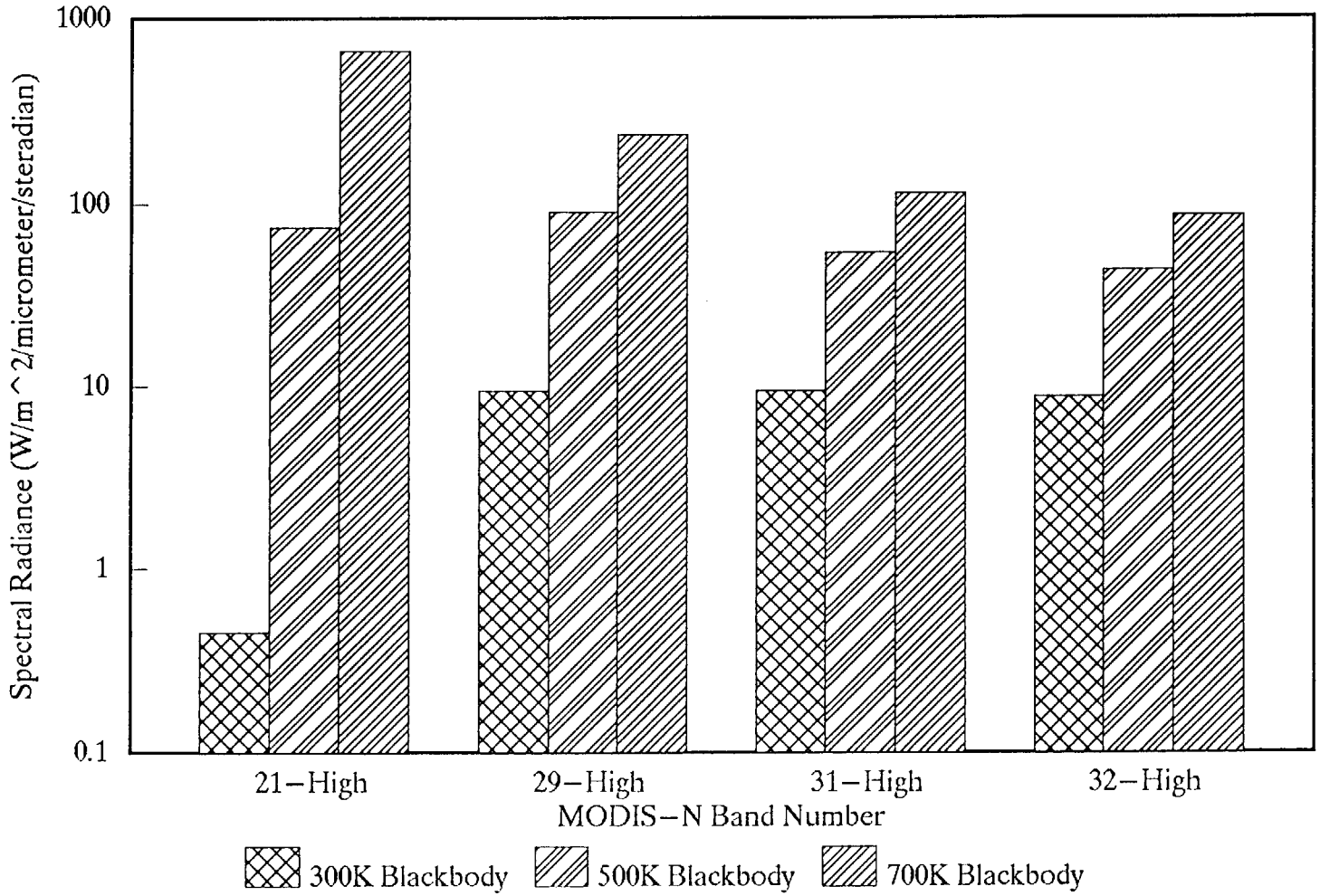

Temperatures are 300, 500, and 700K.

[Computed at center of band]

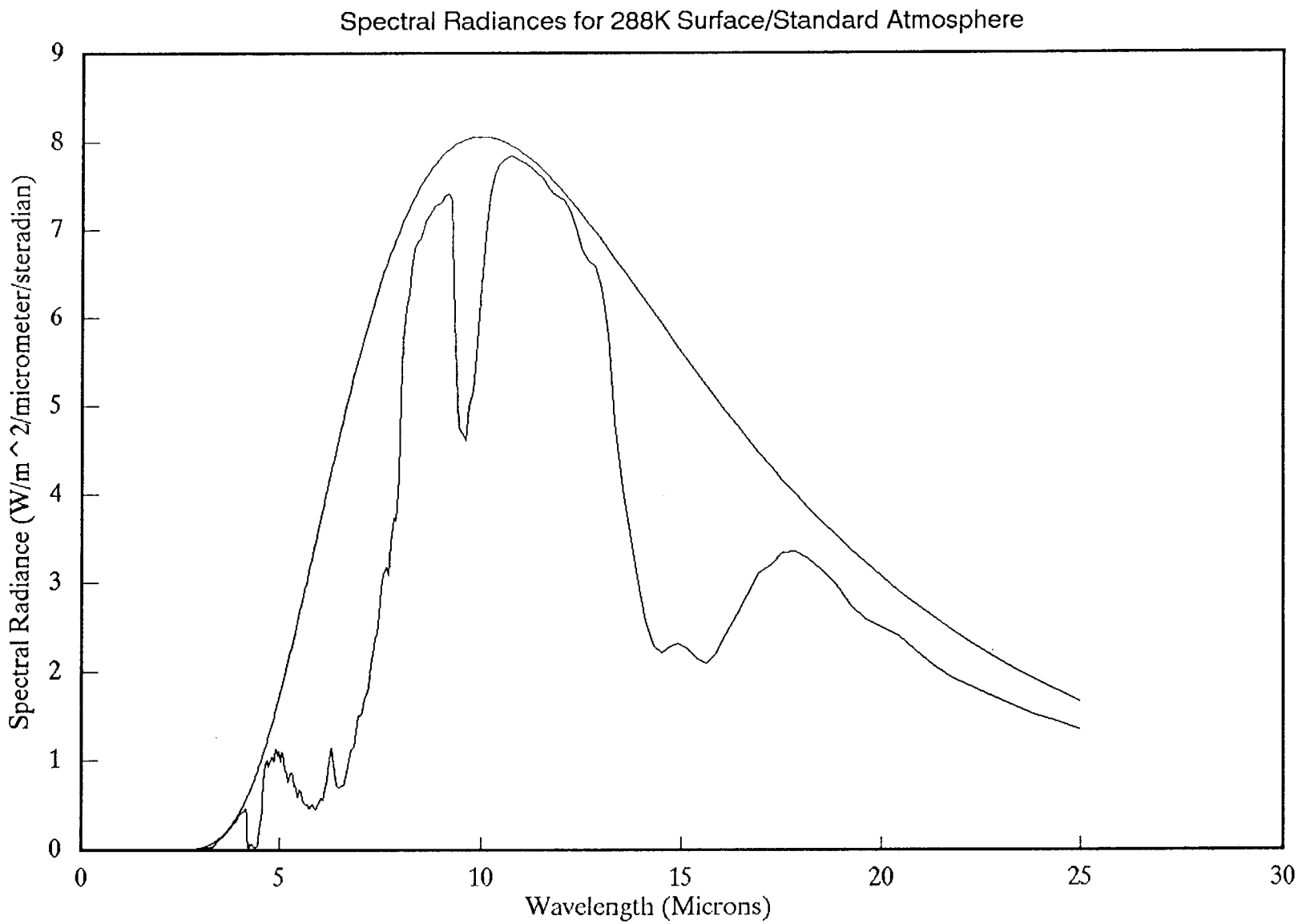

Upper Curve is the Planck 288K Blackbody Radiance
Lower Curve is the 288K Radiance After Passage Through Standard Atmosphere

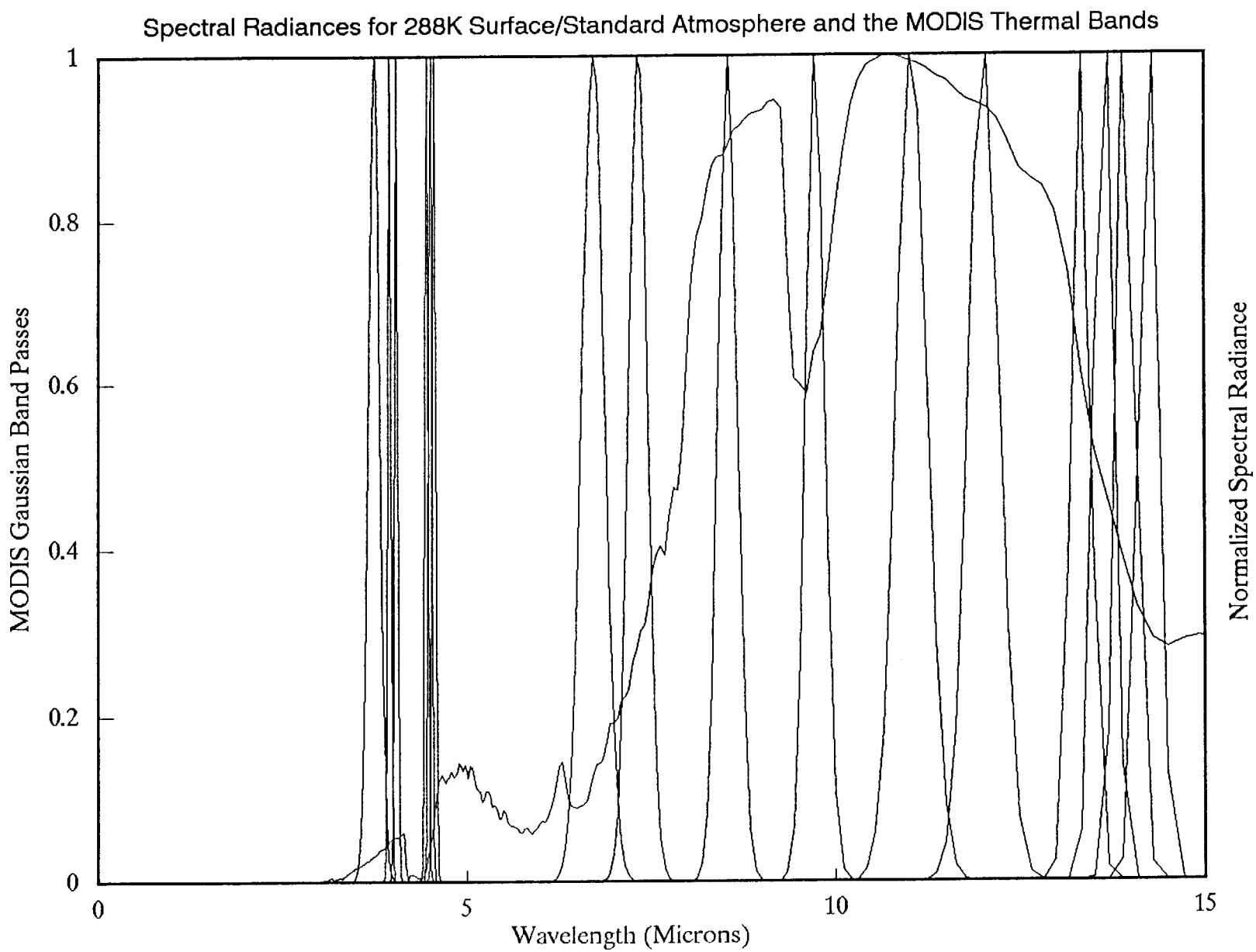
Spectral Radiances for 288K Surface/Standard Atmosphere and the MODIS Thermal Bands
MODIS Gaussian Band Passes
Normalized Spectral Radiance
Wavelength (Microns)
0
0.2
0.4
0.6
0.8
1
0
5
10
15

BAND	CENTER	WIDTH	PURPOSE
21	3.75	0.18	Clouds and Surface Temperature
22	3.96	0.05	Clouds and Surface Temperature
23	4.05	0.05	Clouds and Surface Temperature
24	4.47	0.05	Tropospheric Temperature and Cloud Fraction
25	4.52	0.05	Tropospheric Temperature and Cloud Fraction
26	4.57	0.05	Tropospheric Temperature and Cloud Fraction
27	6.72	0.36	Mid-Tropospheric Humidity
28	7.33	0.30	Upper-Tropospheric Humidity
29	8.55	0.30	Silicate Emissivity; Surface Temperature
30	9.73	0.30	Total Ozone
31	11.03	0.50	Clouds and Surface Temperature
32	12.02	0.50	Clouds and Surface Temperature
33	13.34	0.30	Cloud Height and Fraction
34	13.64	0.30	Cloud Height and Fraction
35	13.94	0.30	Cloud Height and Fraction
36	14.24	0.30	Cloud Height and Fraction

Table 2. Band center (100% response) in microns, full-width half-maximum band width (50% response) in microns, and primary purpose of the 16 MODIS thermal bands.

Chlorophyll Fluorescence Retrieval and its Impact on Atmospheric Corrections

The MODIS atmospheric correction algorithm for water-leaving radiances requires that the ocean water-leaving radiance be zero at specified wavelengths. If the water-leaving radiance is zero at these wavelengths, the aerosol type may be determined and the aerosol contributions to the total radiance can be removed. One of the proposed wavelengths for atmospheric aerosol correction is at 665 nm, which overlaps the signal produced by chlorophyll fluorescence, a MODIS core data product (Figure 1). The fluorescence signal has not been routinely processed by the CZCS, so it may be considered a new satellite product. The question posed here is, will a contribution to water-leaving radiance L_w at 665 nm, where L_w is assumed zero, affect the ability of the atmospheric correction algorithm to retrieve accurate chlorophyll concentrations? A second question is will the fluorescence be retrievable?

To illustrate the problem, we have plotted the normalized water-leaving radiances $[L_w]_N$ over the MODIS-T wavelengths as a function of chlorophyll concentration (Figure 2). These data were generated using the Gordon et al. (1988) expression for $[L_w]_N$ as a function of optical properties, the average cosine (mean path length through the water column) and the extraterrestrial irradiance $F_o(\lambda)$. The optical properties were determined for the chlorophyll concentrations from the model of Sathyendranath and Platt (1988), the average cosine was assumed to be 0.83, and $F_o(\lambda)$ was computed from Bird and Riordan's (1986) mean solar irradiance corrected for Julian Day (assumed = 180; middle of summer) and ozone absorption (assumed scale height .333 atm-cm; Bird and Riordan's ozone absorption coefficients). Mean values at the center of the MODIS bands were assumed. One may note the change in spectral slope between 440 and 550 nm as a function of chlorophyll concentration; it is this difference that gives rise to the ability of satellites to detect chlorophyll.

If chlorophyll fluorescence is occurring, an increase of 0.02% reflectance per mg m^{-3} chlorophyll results (Gower and Borstad, 1983). Given F_o, one may convert this reflectance into an increase in water-leaving radiance, weighted over the spectral bands of MODIS-T (again assuming perfect reception throughout the bandwidth). Figure 3 shows these new radiances for the same chlorophyll concentrations as Figure 2. One notes the increase, especially near 685 nm, but also near 665 nm at high concentrations. The low increase at low concentrations points up the need for high signal-to-noise ratio for fluorescence detection. Since $L_w(665)$ is no longer zero, the question is how will this affect chlorophyll determinations, and should another band be chosen for fluorescence? Secondly, will the fluorescence be detectable if L_w is assumed zero and this increase in L_w is assumed to be aerosol? Thirdly, is there a signal in the aerosol radiances that can be used to detect fluorescence and possibly flag for it in the atmospheric processing?

References

Bird, R.E. and C. Riordan, 1986. Simple solar spectral model for direct and diffuse irradiance on horizontal and tilted planes at the Earth's surface for cloudless atmospheres. Journal of Climate and Applied Meteorology 25: 87-97.

Gordon, H.R., O.B. Brown, R.H. Evans, J.W. Brown, R.C. Smith, K.S. Baker, and D.K. Clark, 1988. A semianalytic radiance model of ocean color. Journal of Geophysical Research 93: 10909-10924.

Gower, J.F.R. and G. Borstad, 1983. Use of the in-vivo fluorescence line at 685 nm for remote sensing surveys of surface chlorophyll a. In: Oceanography from Space. pp. 329-338.

Sathyendranath, S. and T. Platt, 1988. The spectral irradiance field at the surface and in the interior of the ocean: a model for applications in oceanography and remote sensing. Journal of Geophysical Research 93: 9270-9280.

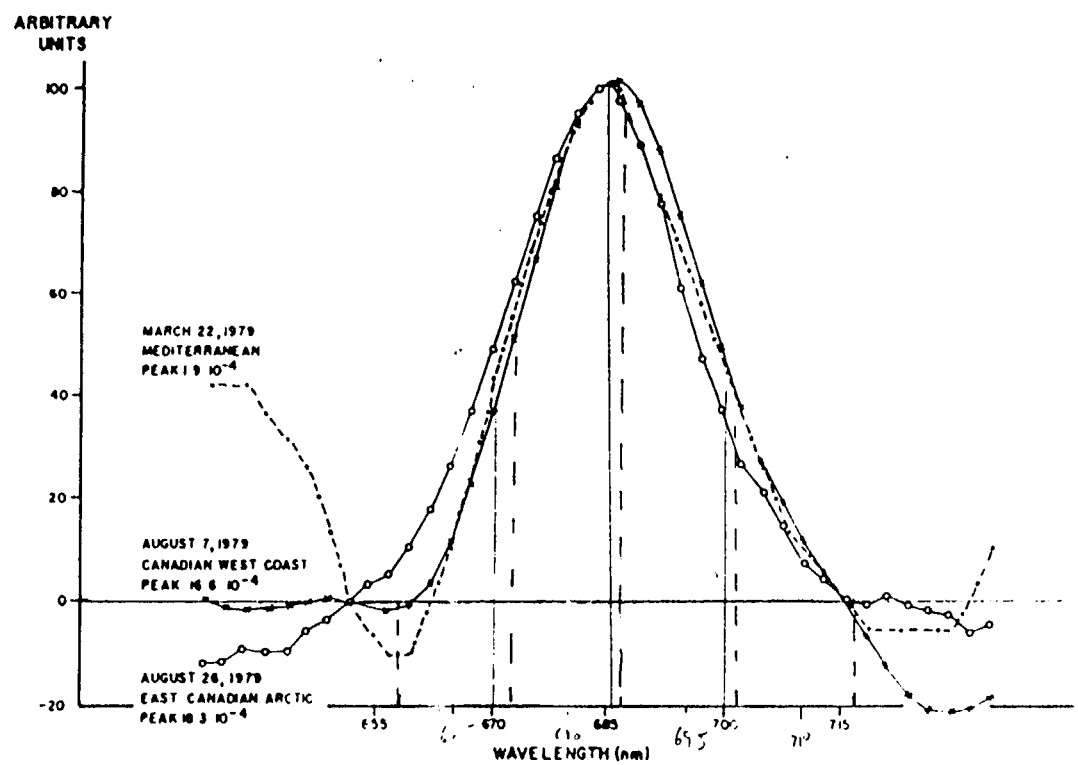

Figure 1. Relative Chlorophyll Fluorescence as a Function of Wavelength

Figure 2. Normalized MODIS-T Water-Leaving Radiances (without Fluorescence)

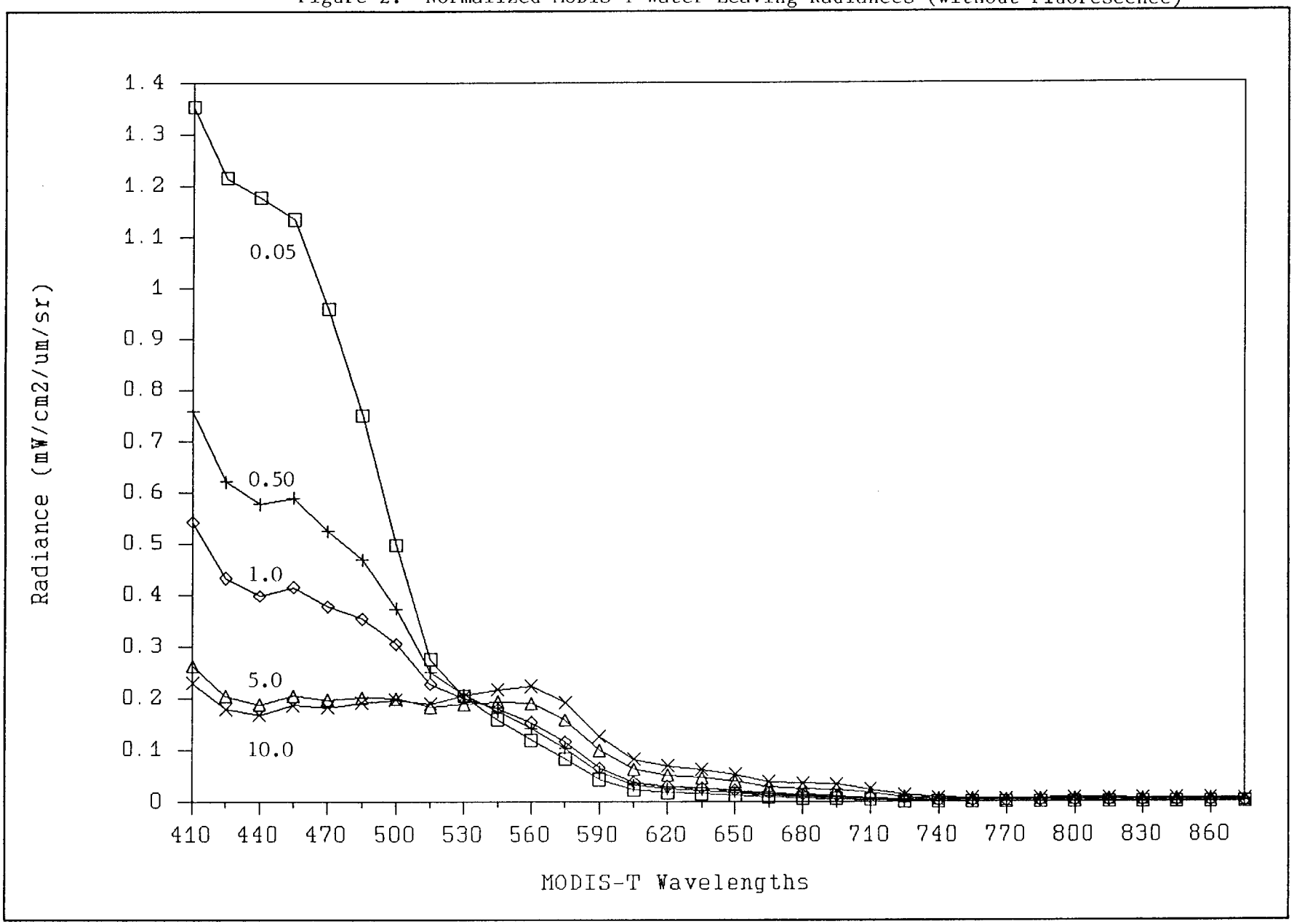

Figure 3. Normalized MODIS-T Water-Leaving Radiances (with Chlorophyll Fluorescence)

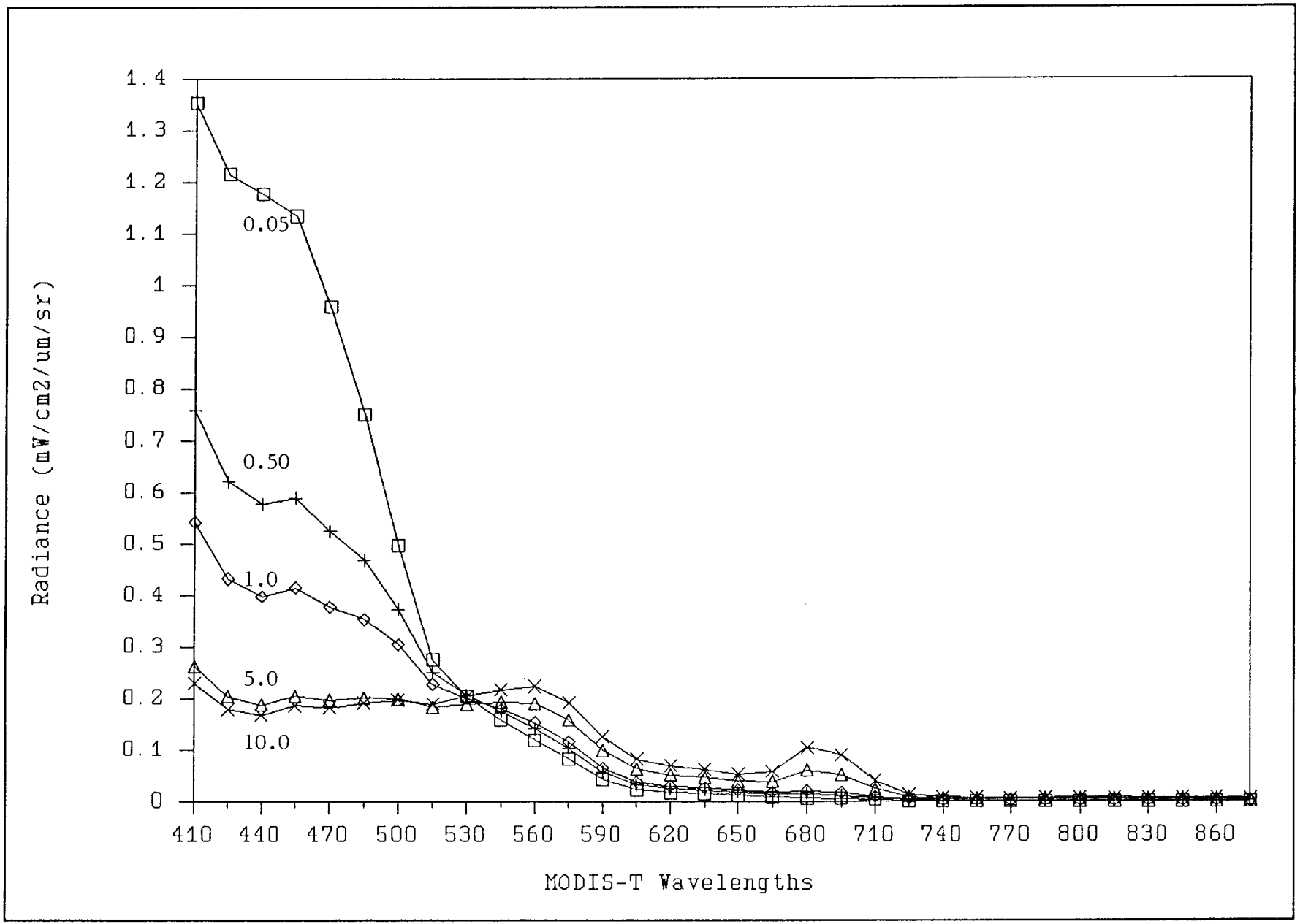

A PRELIMINARY LIST OF MODIS DATA MASKS

Each pixel will have a series of attributes such as elevation, solar zenith angle, and so forth associated with it. These attributes can be calculated each time they are needed or calculated once and stored as masks, which can be considered as slices of a data cube. Masks can be calculated early in the data processing and can be used to direct the flow of subsequent processing or can be used to save computation time if they are used in many algorithms. Many of the masks can be compressed for archival storage. Here is a candidate list of masks with some comments:

GEOMETRIC MASKS

Masks categorized as geometric can be calculated once and used by many algorithms. For example, nearly every algorithm requires knowledge of the solar zenith angle, so, if every team member calculates it, there will not be efficient use of computer resources.

1) Cosine of solar zenith angle and day/night mask

These numbers are used by many algorithms such as the derivation of water leaving radiances, aerosol optical depths, and so forth. The cosine of the angle rather than the angle itself is most commonly used. Since the variation is small from pixel to pixel, this mask can be compressed for long-term storage. If this number is negative, then it is night, so these numbers provide a day/night mask as well.

2) Cosine of satellite zenith angle.

3) Sum of cosine of solar zenith angle and satellite zenith angle

This combination appears to be used by more than one algorithm and may be the mask which is stored.

4) Solar azimuth angle

It is not clear if any team member will use this angle, although in bi-directional models, it is a required number.

5) Satellite azimuth angle

The same comments for the solar azimuth angle apply here.

6) Pixel latitude

It is clear that all team members and the scientific community as a whole requires these numbers. For overcast pixels, this is the latitude of the surface which is calculated from time, satellite location, instrument pointing, and a digital elevation model.

7) Pixel longitude

The same comments for latitude apply to longitude.

8) Pixel elevation and land/ocean mask

If ocean pixels are assigned a number such as -9999., this mask could be used for land/ocean masking. A digital elevation model is required. Given the surface latitude and longitude, the pixel elevation may be found by a table look up procedure.

9) Pixel zenith angle tilt

In steep topography, it may be desirable to have the tilt of the normal vector of the pixel to the vertical angle. The cosine of this angle as for satellite and solar zenith angles may be the parameter to store. It is not clear if the team members have a demand for these numbers. Over oceans, this number is always zero. Presumably given longitude and latitude, this number can be found from a digital elevation model.

10) Pixel azimuth tilt angle

This number tells in what direction the pixel is tilting whereas the zenith angle tilt tells how much the tilt is. Over oceans, this number is always zero.

ATMOSPHERIC MASKS

Many surface parameters require a knowledge of atmospheric conditions so the atmospheric effects can be removed or avoided. It would seem prudent that different algorithms use self-consistent models of the atmosphere. The following masks provide such a mechanism.

1) Pixel cloud cover masks

This could be a single mask resulting from 6 to 10 different cloud cover tests. A cloud / no cloud present would be determined from each test. The test results would be packed into a single word (i.e., single number) to give one mask. Each team member could use the results as they saw fit.

2) Pixel total vertical column ozone

Although this is a core data product derived from the AIRS/AMSU/MODIS instruments, it is also useful as a mask for all ocean products and many atmospheric and land products.

3) Pixel total precipitable water

Derived from AIRS/AMSU/MODIS calculations, these numbers may be useful in atmospheric corrections.

4) Surface pressure mask

This may be derived from surface observations and put into a MODIS format. It is useful in the derivation of ocean data products.

5) Surface wind speed mask

This may be derived from surface observations and put into a MODIS format. It is useful in deriving ocean data products and may have some importance to interdisciplinary investigators who are interested in evapotranspiration over land. SCANSCAT on NPOP-1 may also be a source of this data.

6) Sun glint mask

This is probably derived from the solar zenith angle, satellite zenith angle, and surface wind speed masks combined with the MODIS-T tilt angle. It is probably justified in making it a separate mask.

LAND SURFACE TYPE MASKS

The availability of the following masks will indicate which type of processing may occur for the given pixel. For example, if an ocean pixel is ice covered, further ocean processing may be stopped.

1) Land cover type mask

A map of land cover (e.g., desert, forest, steppe, etc.) may be useful for some processing. It is not clear that such a map exists.

2) Snow-cover and sea ice cover maps

MODIS and other instruments may supply these maps.

3) Coastal ocean mask

Oceans within a certain distance of the coast may be designated as coastal regions. It makes sense to do this once rather than re-determine it for each scene. It could simply be a function of longitude and latitude.

SOME ISSUES RELATING TO CORE MODIS DATA PRODUCTS, ALGORITHMS, AND THEIR PROCESSING SCENARIOS (PARTIAL LIST)

1. **Product Dependencies and Processing Control:** Given that a number of MODIS data products require other MODIS or Eos products as input for their computation, the sequence in which MODIS and other products are generated must be carefully coordinated and controlled. The scheduling and planning problem is not unlike that facing researchers experimenting with parallel computer architectures where output from one processor may be required as input to complete processing at another processor. In fact, many of the techniques developed for parallel computer architectures may be directly applicable to MODIS and other Eos products. While some potentially applicable techniques have been developed, other implementation techniques for parallel systems are currently research topics and results may not be available for MODIS use within the required timeframe.

Issues are as follows: Can techniques developed for parallel computer architectures be applied for MODIS use? Will a complete set of required techniques be available when needed?

2. **Processing redundancy/Product integration:** Since each MODIS Science Team member is individually responsible for only one or a few core data products, and since these products have, in many cases, been developed and validated independently of other MODIS team member efforts, many researchers may initially prefer to implement a complete set of algorithms that generate require data products beginning with MODIS Level-1 data. Since the intermediate products required to generate the required final product may resemble (or be identical to) final core products generated by other team members, processing redundancy may arise. For example, the atmospheric correction currently used for ocean products include aerosol corrections and cloud filters similar to those produced as core products by atmospheric researchers.

The alternative to redundant processing is product integration, which, at least in the case of currently existing products, may require substantial negotiation, algorithm revision, and product revalidation. The basic issues are: How much redundant processing is tolerable? What data system structures would best support the creation of an integrated product set? In the case of cloud products, how much redundancy between the MODIS and CERES efforts is desirable?

3. **Self-consistency of algorithms and their data products:** Aerosol optical depth can be derived by assuming a value for the aerosol single scattering albedo. The aerosol single scattering albedo can be derived independently using MODIS data, although only after a delay of up to 7 to 16 days (for sets of orbits with similar viewing and solar geometries) and only in limited regions. The two data products are not necessarily self-consistent. Will someone impose a requirement for self-consistency? There may be other examples of lack of self-consistency in the MODIS data processing. For example, the MODIS science team may require MODIS-N observations (using the thermal bands) to assist in the identification of clouds for MODIS-T.

4. **Product implementation:** As is the case with other operational satellite data processing systems (e.g., TOVS at NOAA/NESDIS and at INTELSAT), new releases of algorithms are developed, implemented in advanced prototype form, and tested off-line on "parallel" (duplicate) facilities prior to full-scale operational implementation. We advocate the same procedure for MODIS. Furthermore, as with UARS, we advocate the development of an implementation scenario utilizing several releases of simulated data and implementations of the resultant prototype core product algorithms [e.g., preliminary (rough), prototype (full complexity), flight-ready (best as possible before launch; implemented one year before launch), and actual (based on the first several months of MODIS data; implemented 3 to 6 months after launch)].